

See discussions, stats, and author profiles for this publication at: <https://www.researchgate.net/publication/258112358>

# Photofragmentation of the Core-Excited s-Tetrazine Molecule Near the Carbon and Nitrogen K Edges

ARTICLE *in* THE JOURNAL OF PHYSICAL CHEMISTRY A · FEBRUARY 1995

Impact Factor: 2.69 · DOI: 10.1021/j100006a015

---

CITATIONS

7

---

READS

7

4 AUTHORS, INCLUDING:



Marc Simon

Pierre and Marie Curie University - Paris 6

163 PUBLICATIONS 1,820 CITATIONS

SEE PROFILE

# Photofragmentation of the Core-Excited *s*-Tetrazine Molecule near the Carbon and Nitrogen K Edges

Marc Simon,<sup>†,‡</sup> Michel Lavollée,<sup>†</sup> Paul Morin,<sup>†,‡</sup> and Irène Nenner<sup>\*,†,‡</sup>

LURE, Laboratoire mixte CNRS, CEA et MESR, Centre Universitaire, Bâtiment 209D, 91405 Orsay Cedex, France, and CEA, Service des Photons, Atomes et Molécules, Bâtiment 522, 91191 Gif sur Yvette Cedex, France

Received: August 5, 1994; In Final Form: October 10, 1994<sup>®</sup>

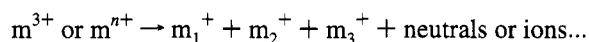
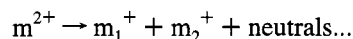
Total photoionization spectra of *s*-tetrazine have been measured with soft X-ray synchrotron radiation, in the vicinity of the nitrogen and carbon 1s edges. Multicoincidence time of flight mass spectrometry measurements show that the core-excited or -ionized molecule undergoes a cascade of dissociative double and triple ionization, causing the formation of numerous atomic and diatomic ionic and neutral fragments including N<sub>2</sub> and HCN. Several routes leading to two-, three-, and many-body dissociation reactions with the CN<sub>2</sub>H<sup>+</sup>, C<sub>2</sub>N<sub>3</sub>H<sub>2</sub><sup>2+</sup>, and C<sub>2</sub>N<sub>2</sub>H<sub>2</sub><sup>2+</sup> intermediates are discussed. The results are consistent with the formation of a wide electron energy distribution and significant internal energy in the residual ion and nascent primary fragments. The role of multistep dissociative autoionization in the single-, double-, and triple-ionization continua is discussed, including the statistical dissociation of intermediate ion fragments. The absence of site selectivity is discussed in terms of charge delocalization, symmetry considerations, efficiency of the multifragmentation, and possible statistical fragmentation steps.

## I. Introduction

The investigation of the fragmentation of core-excited molecules using tunable synchrotron radiation has been the subject of many studies in recent years because it is one of the basics of direct radiation damage phenomena and also because it is relevant to other fields such as photodesorption of surfaces, technology (photoetching, lithography, photon-induced vapor deposition), radiobiology, and even interstellar photochemistry.<sup>1</sup> The existence of possible site selective fragmentation processes after core photoexcitation has motivated numerous studies<sup>2–26</sup> in small model diatomic and triatomic molecules, halogeno and other hydrocarbons, and organometallic and silicon compounds. Such effects indeed exist, but a great variety of situations are found, including the total loss of memory of the initially excited site. It is known that multiionization due to the electronic relaxation of the core hole plays a major role to dissociate the system efficiently,<sup>1</sup> but the dynamics of the fragmentation is found to be quite complex, especially in medium size molecules. On short (femtosecond) time scales, the direct fragmentation<sup>4,7,8</sup> competes with the electronic relaxation of the core hole (known as autoionization or resonant Auger) because of strong repulsion of the electronic clouds around each fragment in the early stage of the photoexcitation<sup>21,22</sup> and/or because of Coulombic repulsion after the ejection of several electrons. At longer times, cascades of fragmentation expected from statistical theory<sup>27</sup> probably occur, but neither the role of charge of the molecular parent (or fragment ion) nor the role of Coulombic repulsion is clearly established.

In the present article, we investigate the problem of multifragmentation in the *s*-tetrazine molecule, C<sub>2</sub>N<sub>4</sub>H<sub>2</sub>, after excitation in the soft X-ray region, namely, the 285–320 eV (carbon 1s excitation) and 395–435 eV (nitrogen 1s excitation) ranges. This is the first aromatic system ever investigated under soft X-ray irradiation, and it is of direct relevance to the problem of survival of polycyclic aromatic molecules as a model for dust

in the region of star formation<sup>28</sup> and to the possible role of inner-shell ionization phenomena in the DNA of cell inactivation by heavy ions.<sup>29</sup> In contrast to acyclic systems, one of the important fragmentation steps is the opening of the ring, and it is interesting to know if this process is part of a sequential dissociation cascade or is a concerted process involving the breaking of several bonds such as C–N or N–N. Secondly, this molecule is known to fragment efficiently (three body) but in a different fashion in the visible,<sup>30</sup> near,<sup>31</sup> and far<sup>32</sup> ultraviolet region, and these previous results together with the present work offer a complete set of photochemistry processes over an extended photon energy range. Our recent work on the *s*-tetrazine molecular ion,<sup>32</sup> C<sub>2</sub>N<sub>4</sub>H<sub>2</sub><sup>2+</sup>, produced by one-photon double ionization near threshold of the neutral molecule, is of special relevance for the present work because it deals with the fragmentation of the dication into two-, three-, and more-body reactions. Furthermore, the same experimental method, namely, time of flight mass spectrometry operated in the multicoincidence mode (known as the photoelectron photoion photoion coincidence, PEPICO, method or charge separation mass spectrometry, CSMS) has been used.<sup>33,34</sup> Here, we report measurements of a number of multifragmentation processes in this core-excited molecule, of the following type:



leading to a quasi explosion of the molecule into many atomic or diatomic fragments because of double, triple, and multiionization and a cascade of sequential fragmentations. We discuss the role of dissociative autoionization and the lack of site selectivity between the carbon and nitrogen 1s excitations.

## II. Experimental Section

We have used the charge separation mass spectrometry technique to measure the fragmentation of a molecular ion into two (photoelectron photoion photoion coincidence, PEPICO)

<sup>†</sup> LURE.

<sup>‡</sup> CEA.

<sup>®</sup> Abstract published in *Advance ACS Abstracts*, January 15, 1995.

or three (photoelectron triple photoion coincidence, PE3PICO) singly charged positive fragment ions.

The apparatus, briefly presented here, is described in detail elsewhere.<sup>35</sup> Synchrotron radiation on the SU7 beam line of the Super ACO storage ring at LURE, Orsay, in the 200–800 eV photon energy range is used. This allows us access to the carbon (around 290 eV) and nitrogen K edges (around 410 eV). A grazing incidence monochromator equipped with three interchangeable toroidal gratings<sup>37</sup> provides radiation with an energy resolution of 0.25 eV at 250 eV with slit widths of 40  $\mu\text{m}$  (entrance slit) and 60  $\mu\text{m}$  (exit slit). The monochromatic photon beam is refocused by a toroidal mirror at the center of the ionization chamber of a time of flight mass spectrometer. A dc electric field of 2 kV/cm deflects electrons and ions in opposite directions. Electrons are detected without energy analysis by a set of channelplates giving the start pulse for the coincidence experiment. Fragment ions are mass analyzed into a 12 cm drift tube and detected by channelplates. The incident photon flux is measured in a separate experiment by recording the total ion yield of argon.

Measurements of multicoincidences are summarized as follows. For a given event, one detects, within a time window of 2.5  $\mu\text{s}$  (a time slightly longer than the time of flight of the parent ion), the fragment ions as a function of their time of flight. At present, we are able to detect the arrival of three correlated fragment ions. One obtains simultaneously

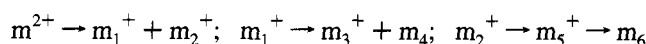
(i) one-dimensional time of flight spectra for simple correlation between one electron and one ion (PEPICO);

(ii) two-dimensional spectra for double correlations between one electron and two fragment ions (PEPIPICO);

(iii) three-dimensional spectra for triple correlation between one electron and three ions (PE3PICO).

The counting rate is kept low in order to reduce fortuitous coincidences. In the present work, we have 1500 simple coincidence events per second. Due to the limited collection efficiency of the detector, we could record 250 c/s for PEPICO and 50 c/s for PE3PICO. The PEPICO data are compressed in the form  $(z, t_1, t_2)$  where  $z$  is the number of occurrences of the ion pair 1, 2. We reject double-coincidence events for  $z = 1$  and stop the double-coincidence counting after 50 000 total double-coincidence events. A sophisticated method for subtracting such false coincidences has been described by Frasnisky et al.<sup>33</sup> Most of the false double coincidences (PEPIPICO) are due to the accidental correlation of one true ion and another ion (noncorrelated with the same electron). In the present case, the false coincidence rate is considered negligible because the double-ionization cross sections are much higher than in ref 32, for which double-ionization measurements have been performed near threshold. We also reject any event  $(z, t_1, t_2)$  for which one of the two ions 1 or 2 is not detected in the simple coincidence spectrum. The final true double-coincidence spectrum is presented in a two-dimension contour plot  $(z, t_1, t_2)$ . In the present paper, we rely on the shape (stick, parallelogram, or oval and their respective slopes) of the peaks<sup>38,39</sup> to learn about the dissociation mechanism. Two-body reactions always appear as a stick with a  $-1$  slope because the momenta of the fragments are anticorrelated. For three-body reactions, various shapes (oval, parallelogram, and more complex situations) are usually found. Stepwise reactions can be distinguished from concerted one-step reactions by observing parallelogram shapes<sup>38</sup> as opposed to oval shapes. Among stepwise reactions, deferred charge separation (loss of neutral fragment preceding charge separation) can be distinguished from secondary decay (loss of neutral after charge separation) from the slope of the pattern. A slope of  $-1$  can be the sign of a

deferred charge separation reaction or a concerted reaction. A slope markedly different from the  $-1$  value generally indicates a secondary reaction. If the intermediates survive for a period larger than one rotation, the slope equals the ratio of the ionic fragment mass over the mass of the intermediate ion, and this helps to identify the sequence. If the intermediates survive much less than one rotation, the slope is smaller than the latter value, and a definite identification and evaluation of the angular correlations of the particle momenta requires Monte Carlo simulations.<sup>32</sup> In cases of cascades of secondary dissociations, the slope of the pattern can be interpreted using the mass of intermediates and final ionic fragments.<sup>35</sup> Here, we made only a first-order analysis without simulations, assuming that spurious coincidences do not affect seriously the shape of the peak. Those spurious coincidences originate from the ion detection efficiency which is less than unity. For example, they are due to dissociative triple-ionization events for which one of the three ions has not been detected. Here, the situation is very complex, and such corrections are impossible to make, especially for ion pairs with the same mass for which the dead time of 7 ns of the detection system prevents observation of the full shape of the pattern. We then assume that the kinetic energy released for two-body reactions or stepwise three-body reactions extracted respectively from the stick length and parallelogram length and width is reliable. For a complex secondary decay such as



the slope of the  $m_3^+, m_5^+$  peak gives the mechanism, but one cannot extract the kinetic energy release of primary and secondary steps from the pattern.<sup>25</sup>

PE3PICO data are compressed in the form  $(z, t_1, t_2, t_3)$ . Hence, the problem of false coincidences becomes crucial because about 40% are false. We reject all coincidences for which at least one of the ions with time of flight  $t_1, t_2$ , or  $t_3$  does not appear in the simple coincidence spectrum and does not correspond to a real fragment. Since visualization of such triple coincidences are difficult to present on a multidimensional basis, we simply show them on a one-dimension plot  $(z, t_1 + t_2 + t_3)$ . Indeed, in a three-body reaction,  $m^{3+} \rightarrow m_2^+ + m_3^+$ , the sum  $(t_1 + t_2 + t_3)$  is a constant because the momentum conservation law implies  $P_1 + P_2 + P_3 = 0$ . In a  $(z, t_1, t_2 + t_3)$  plot, it appears as a sharp peak. When a fourth particle is created or a multiply charged fragment is produced, the peak is widened because  $P_1 + P_2 + P_3 \neq 0$ . Assignment of each peak is made by knowing the time of flight of each ion as measured in the simple coincidence spectrum.

The *s*-tetrazine sample was synthesized by the method of Antonius et al.<sup>40</sup> in the laboratory. It was heated at a temperature of 40  $^\circ\text{C}$  to increase the vapor pressure. The measurements were performed with a dynamical pressure of  $8 \times 10^{-6}$  Torr in the chamber.

### III. Results and Discussion

**A. Total Photoionization Spectra.** We present, in Figure 1, the total ion yield of *s*-tetrazine, as a function of photon energy in the region of the carbon and nitrogen K edges. Such spectra mimic the photoabsorption spectra of the molecule. The nitrogen K spectrum is spoiled by a signal of gaseous  $\text{N}_2$ , due to a small leak in the inlet system. On the basis of the relative photoabsorption cross section of  $\text{N}_2$ , we could identify the  $\pi^*$  peak of  $\text{N}_2$  at 401 eV and used it for energy calibration around the nitrogen edge. The energy calibration around the carbon edge has been made by assuming that the first  $\pi^*$  resonance is located at 285.4 eV, as for pyridine,<sup>41</sup> since the  $\pi^*$  resonance

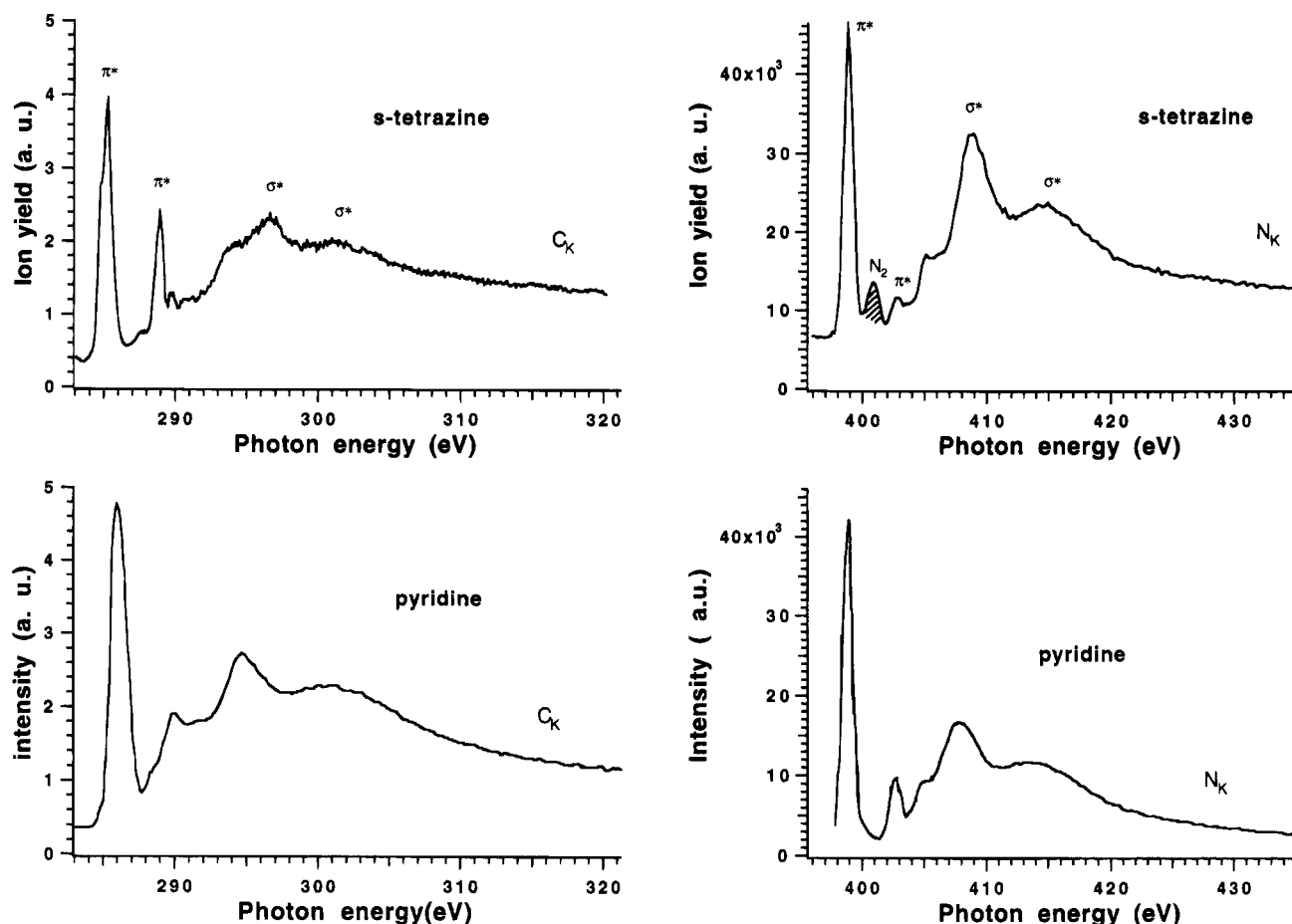


**Figure 1.** Soft X-ray total ionization spectra of the gas phase *s*-tetrazine molecule, near the carbon and nitrogen K ionization edges (this work). Comparison with the  $C_K$  and  $N_K$  inner shell electron energy loss spectra of pyridine reproduced from Horsley et al.<sup>41</sup>

energy at the nitrogen edge, after independent calibration, is found at the same value as for pyridine.

We compare the present results with the experimental electron energy loss spectrum of pyridine,  $C_5H_5N$ , as measured by Horsley et al.<sup>41</sup> (see Figure 1) because it is an isoelectronic aromatic system and also the simplest N-heterocyclic-related molecule. There is a striking resemblance between the  $C_{1s}$  and  $N_{1s}$  spectra of pyridine and *s*-tetrazine. There is also a strong similarity between the  $C_{1s}$  spectra of the two N-heterocyclic molecules and the benzene spectrum (not shown here; see ref 42). The first and second intense resonances observed in both the carbon and nitrogen spectrum are due to the core to  $\pi^*$  transitions, following the theoretical calculations on benzene.<sup>43</sup> The symmetry breaking with respect to benzene, as originated from the CH substitution by nitrogen atoms, is expected to remove the degeneracy of the first  $C_{1s} \rightarrow \pi^*$  ( $e_{2u}$ ) resonance in benzene,<sup>44,45</sup> but our present photon energy resolution is not sufficient to observe it. Other weak features in the discrete region are probably due to Rydberg states, and their precise assignment requires extensive calculations. In the continuum, one observes three resonances, the position of two of which match quite well those observed in the pyridine spectrum. Located in the  $C_{1s}$  spectrum at 296.8 and 322 eV and in the  $N_{1s}$  spectrum at 408 and 414 eV, these are very probably  $\sigma^*$  resonances, following the theoretical calculations of the benzene spectrum.<sup>41</sup> The third one located at 294 and 405 eV, respectively, in the  $C_{1s}$  and  $N_{1s}$  spectra is more difficult to interpret in the absence of multiple scattering calculations. Nevertheless, it is interesting to observe that these structures, which are observed in pyridine, are enhanced relative to the

**TABLE 1: Mass Spectrum of *s*-Tetrazine at 285.2 eV ( $C_{1s} \rightarrow \pi^*$ ) Photon Energy**

$m/z$	identification	relative intensity (% of the total)
1	$H^+$	20.4
12	$C^+$	10.2
13	$CH^+$	12.5
14	$N^+$	9.5
15	$HN^+$	1.8
26	$CN^+$	10.4
27	$HCN^+$	22.3
28	$N_2^+, HCNH^+$	7.8
29	$HN_2^+$	1.3
40	$CN_2^+$	1.3
41	$HCN_2^+$	1.5
53	$HC_2N_2^+$	0.5
55	$HC_2N_3^+$	0.5

first  $\pi^*$  resonance intensity. This shows the role played by the number of nitrogen atoms, which is increased by a factor of 4 in the present molecule. Bearing in mind that the valence excitation transitions of nonbonding electrons into the unoccupied levels ( $n \rightarrow \pi^*$ ) are strong in N-heterocyclic molecules,<sup>46</sup> it is possible that such features are due to the breakdown of the independent particle model. In other words, core excitation is accompanied by valence excitation, as commonly observed in many molecules (see for example the  $N_2$  case in ref 47).

**B. Mass Spectra.** A conventional mass spectrum of *s*-tetrazine is obtained by simple photoelectron photoion coincidence measurements. The results obtained at 285.2 eV are presented in Table 1. Very similar results are obtained in the region of the carbon and nitrogen edges and on and off resonance. The striking point is that the sizes of fragments are

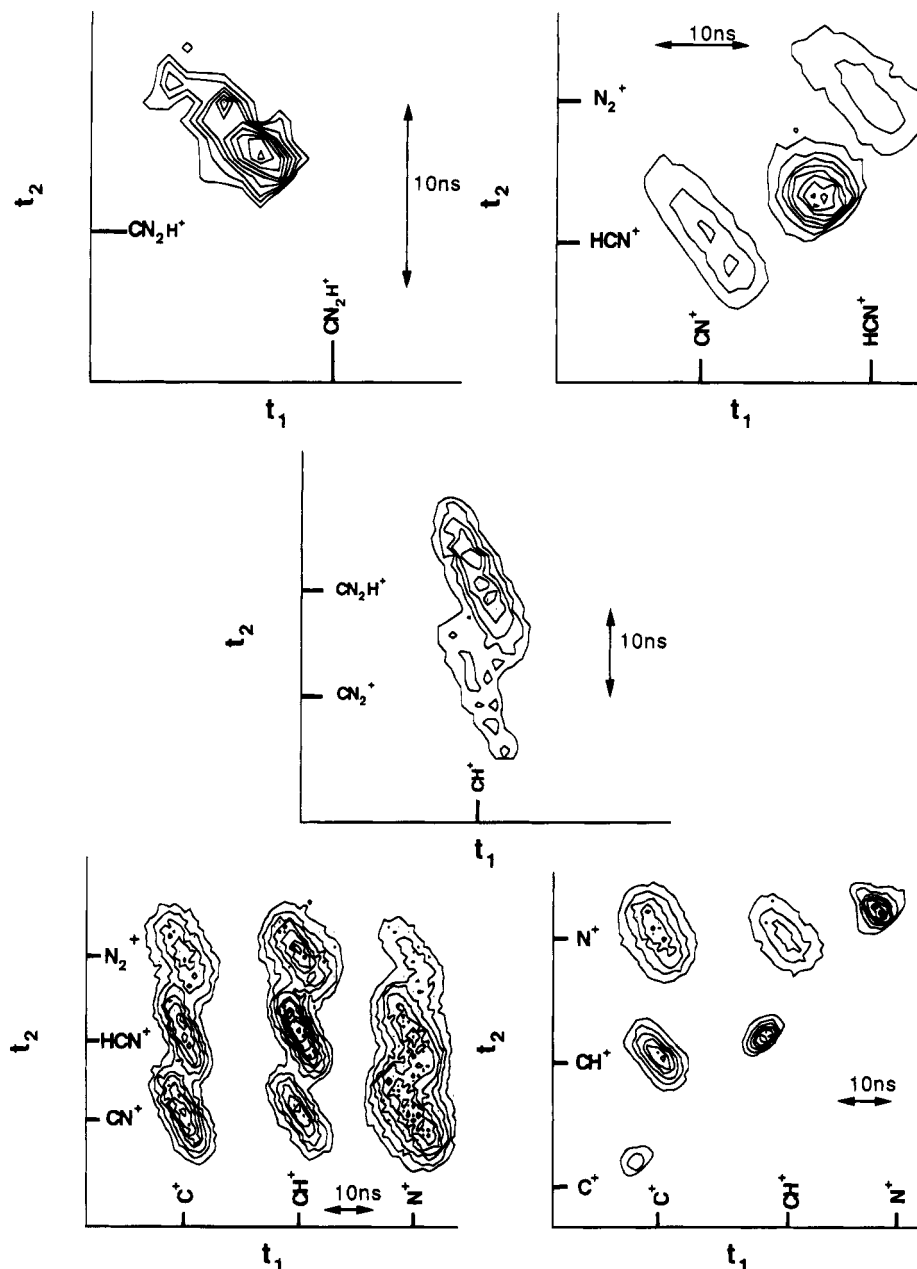


**Figure 2.** 2D charge separation mass spectra of selected ion pairs. The time of flight scales (horizontal and vertical) are identical for each diagram.

mostly atomic and diatomic, and only a very few polyatomic fragments are observed. Interestingly, the  $\text{HN}^+$ ,  $\text{HCNH}^+$ , and  $\text{HN}_2^+$  fragments must originate from rearrangement, i.e. a proton transfer from carbon to nitrogen, since there is not N–H bond in the original neutral molecule. Other fragments may also be arranged due to C,N scrambling, but the present measurements do not give any spectroscopic or geometrical information. The fragmentation pattern is found to be quite similar from one edge to the other. The difference between the relative intensity of each relative peak intensity ( $\text{C}_{1s} \rightarrow \pi^*$  compared to the  $\text{N}_{1s} \rightarrow \pi^*$  resonances and  $\text{C}_{1s} \rightarrow \sigma^*$  compared to the  $\text{N}_{1s} \rightarrow \sigma^*$ ) never exceeds 3%. This strong similarity reflects that the residual molecular ions (with a certain distribution of positive charges) are similar in nature and in internal energy, independently of the location of the initial core hole vacancy. This loss of memory of the excitation site is discussed below.

**C. Multicoincidence Measurements and Fragmentation Mechanisms.** PEPICO spectra have been measured at the  $\pi^*$  and  $\sigma^*$  resonances near the carbon and nitrogen edges.

Qualitatively, there is no change in the nature of coincidence peaks from one energy to the other except that the overall intensity of the spectrum is clearly enhanced from  $\pi^*$  to  $\sigma^*$  resonances. Therefore, we have added all spectra recorded at different photon energies to the resonances near the carbon and nitrogen edges, to increase the total counts and thus improve the statistics, in order to approach the fragmentation mechanisms. We show in Figure 2 the contours in the  $t_1, t_2$  plane for selected ion pairs associated with two-, three-, and many-body reactions. The peaks  $(1^+, 12^+)$ ,  $(1^+, 13^+)$ ,  $(1^+, 14^+)$ ,  $(1^+, 15^+)$ ,  $(1^+, 26^+)$ ,  $(1^+, 27^+)$ ,  $(1^+, 28^+)$ ,  $(1^+, 29^+)$ ,  $(1^+, 40^+)$ ,  $(1^+, 41^+)$ ,  $(1^+, 53^+)$ , and  $(1^+, 55^+)$  associated with  $(\text{H}^+, \text{C}^+)$ ,  $(\text{H}^+, \text{CH}^+)$ ,  $(\text{H}^+, \text{N}^+)$ ,  $(\text{H}^+, \text{NH}^+)$ ,  $(\text{H}^+, \text{CN}^+)$ ,  $(\text{H}^+, \text{HCN}^+)$ ,  $(\text{H}^+, \text{N}_2^+)$ ,  $(\text{H}^+, \text{N}_2\text{H}^+)$ ,  $(\text{H}^+, \text{CN}_2^+)$ ,  $(\text{H}^+, \text{CN}_2\text{H}^+)$ ,  $(\text{H}^+, \text{C}_2\text{N}_2\text{H}^+)$ , and  $(\text{H}^+, \text{CN}_3\text{H}^+)$  are not shown, although altogether they represent some 53% of the total coincidence counts. This is because their peak shape cannot be analyzed due to the difficulty of accounting for the instrumental time broadening for correlated fragments with very different masses. The  $(27^+, 55^+)$ ,  $(29^+, 53^+)$ ,

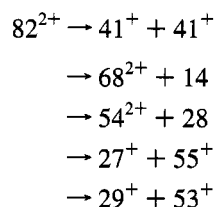
(27<sup>+</sup>,40<sup>+</sup>), (27<sup>+</sup>,41<sup>+</sup>), (12<sup>+</sup>,40<sup>+</sup>), (12<sup>+</sup>,41<sup>+</sup>), and (14<sup>+</sup>,40<sup>+</sup>) peaks, which are due to (HCN<sup>+</sup>,C<sub>2</sub>N<sub>2</sub>H<sup>+</sup>), (N<sub>2</sub>H<sup>+</sup>,CN<sub>3</sub>H<sup>+</sup>), (HCN<sup>+</sup>,CN<sub>2</sub><sup>+</sup>), (HCN<sup>+</sup>,CHN<sub>2</sub><sup>+</sup>), (C<sup>+</sup>,CN<sub>2</sub><sup>+</sup>), (C<sup>+</sup>,CN<sub>2</sub>H<sup>+</sup>), and (N<sup>+</sup>,CN<sub>2</sub><sup>+</sup>), are also not shown, because of the very low signal to noise ratio.

The overall PEPICO results show that all fragments of the mass spectrum (Table 1) are correlated and are involved in double and most probably triple ionization. Among the numerous correlated fragments, we have chosen to establish the fragmentation mechanism on selected cases showing a high signal to noise ratio, a clear-cut parallelogram shape, and on the basis of the following criteria.

(i) We have not considered pairs of ions with the same mass which show a truncated pattern. In addition, if spurious triple coincidences are significant in the double-coincidence signal, the resulting pattern would be closer to an ellipse because of the superposition of two parallelograms with different slopes.<sup>48,49</sup>

(ii) We have not deduced any mechanism from peaks for heavier masses together with H<sup>+</sup> because the difference of masses with H<sup>+</sup> makes the shape of the pattern obtained under high extraction field conditions impossible to analyze.

Using the method for sequential dissociation mechanisms based on momentum conservation law for three-body<sup>34</sup> and generalized to four-body<sup>25</sup> reactions, we have interpreted the slope of various coincidence peaks and suggested sequential mechanisms as reported in Table 2, restricting the pathways to those giving the closest slope to the observations. It is interesting to observe that the first step of three- and many-body reactions is one of the two-body reactions:



All of them have been observed near the double-ionization threshold<sup>32</sup> except the loss of N. The charge separation reactions mentioned above are directly observed. In contrast, the 68<sup>2+</sup> (as well as 54<sup>2+</sup>) peak is absent in the mass spectrum, but its fragmentation is found to be the route to produce several smaller fragments. Taking the (13<sup>+</sup>,41<sup>+</sup>) peak as an example, we find that sequential dissociation via the formation of 68<sup>2+</sup> gives a satisfactory slope (Table 2). However, we cannot rule out the alternative mechanism, 82<sup>2+</sup> → 41<sup>+</sup> + 41<sup>+</sup>; 41<sup>+</sup> → 13<sup>+</sup> + 28. The corresponding slope of the peak would be equal to -3.15, but if the CHN<sub>2</sub><sup>+</sup> intermediate dissociates with a small kinetic energy release along the line of charge separation, the slope may be smaller than expected.<sup>32</sup> The same reasoning is true for the (27<sup>+</sup>,41<sup>+</sup>) or the (26<sup>+</sup>,27<sup>+</sup>) pair. Simulations are needed to clarify this point.

The similarity of the present kinetic energies released for two-body charge separation reactions to those found near threshold implies that, in the core hole relaxation processes, double ionization leads to the production of the parent dication with a similar internal distribution. This is indeed possible if we rely on the electronic deexcitation spectra performed on azabenzene molecules in thin films condensed onto a copper single-crystal substrate measured by Eberhardt et al.<sup>50</sup> Those molecules are aromatic species with one (pyridine), two (pyrazine), and three (*s*-triazine) nitrogens atoms in the aromatic ring, all of them being isoelectronic to the present molecule. According to Eberhardt et al.,<sup>50</sup> the electronic deexcitation spectra of the N<sub>1s</sub> core-ionized (Auger spectrum) and core-excited (core → π\*)

**TABLE 2: Two-, Three-, and Many-Body Reactions in *s*-Tetrazine As Extracted from the Peak Shape of Selected Ion Pairs in Double-Coincidence Spectra**

reaction type	ion pair	measured slope	suggested mechanism	calculated slope
two body	(27 <sup>+</sup> ,55 <sup>+</sup> )	-1	82 <sup>2+</sup> → 27 <sup>+</sup> + 55 <sup>+</sup> KER = 3 eV ± 1	-1
	(29 <sup>+</sup> ,53 <sup>+</sup> )	-1	82 <sup>2+</sup> → 29 <sup>+</sup> + 53 <sup>+</sup> KER = 3 eV ± 1	-1
	(41 <sup>+</sup> ,41 <sup>+</sup> )	-1	82 <sup>2+</sup> → 41 <sup>+</sup> + 41 <sup>+</sup> KER = 4.5 eV ± 1	-1
three body	(27 <sup>+</sup> ,41 <sup>+</sup> )	-1	82 <sup>2+</sup> → 68 <sup>2+</sup> + 14 KER = 0.6 eV 68 <sup>2+</sup> → 27 <sup>+</sup> + 41 KER = 2.4 eV	-1
			82 <sup>2+</sup> → 41 <sup>+</sup> + 41 <sup>+</sup> 41 <sup>+</sup> → 27 <sup>+</sup> + 14	-1.52
many body	(26 <sup>+</sup> ,27 <sup>+</sup> )	-1.35	82 <sup>2+</sup> → 68 <sup>2+</sup> + 14 68 <sup>2+</sup> → 27 <sup>+</sup> + 41 <sup>+</sup> 41 <sup>+</sup> → 26 <sup>+</sup> + 15	-1.58
			82 <sup>2+</sup> → 54 <sup>2+</sup> + 28 54 <sup>2+</sup> → 27 <sup>+</sup> + 27 <sup>+</sup> 27 <sup>+</sup> → 26 <sup>+</sup> + 1	-1.03
			82 <sup>2+</sup> → 41 <sup>+</sup> + 41 <sup>+</sup> 41 <sup>+</sup> → 28 <sup>+</sup> + 13 41 <sup>+</sup> → 27 <sup>+</sup> + 14	-1.03
	(27 <sup>+</sup> ,28 <sup>+</sup> )	-1.15	82 <sup>2+</sup> → 41 <sup>+</sup> + 41 <sup>+</sup> 41 <sup>+</sup> → 28 <sup>+</sup> + 13 41 <sup>+</sup> → 27 <sup>+</sup> + 14	-1.04
			82 <sup>2+</sup> → 27 <sup>+</sup> + 28 <sup>+</sup> + 27 82 <sup>2+</sup> → 41 <sup>+</sup> + 41 <sup>+</sup> 2 × (41 <sup>+</sup> → 27 <sup>+</sup> + 14) 27 <sup>+</sup> → 13 <sup>+</sup> + 14	-1 -2.08
			82 <sup>2+</sup> → 41 <sup>+</sup> + 41 <sup>+</sup> 41 <sup>+</sup> → 27 <sup>+</sup> + 14 41 <sup>+</sup> → 13 <sup>+</sup> + 28	-2.08
	(13 <sup>+</sup> ,27 <sup>+</sup> )	-1.92	82 <sup>2+</sup> → 54 <sup>2+</sup> + 28 54 <sup>2+</sup> → 27 <sup>+</sup> + 27 <sup>+</sup> 27 <sup>+</sup> → 13 <sup>+</sup> + 14	-2.08
			82 <sup>2+</sup> → 68 <sup>2+</sup> + 14 68 <sup>2+</sup> → 27 <sup>+</sup> + 14 <sup>+</sup> 27 <sup>+</sup> → 13 <sup>+</sup> + 14	-2.08
			82 <sup>2+</sup> → 41 <sup>+</sup> + 41 <sup>+</sup> 41 <sup>+</sup> → 13 <sup>+</sup> + 28 82 <sup>2+</sup> → 68 <sup>2+</sup> + 14 68 <sup>2+</sup> → 27 <sup>+</sup> + 41 <sup>+</sup> 41 <sup>+</sup> → 40 <sup>+</sup> + 1 27 <sup>+</sup> → 13 <sup>+</sup> + 14	-3.15 -2.03
	(13 <sup>+</sup> ,41 <sup>+</sup> )	-2.1	82 <sup>2+</sup> → 41 <sup>+</sup> + 41 <sup>+</sup> 41 <sup>+</sup> → 13 <sup>+</sup> + 28 82 <sup>2+</sup> → 68 <sup>2+</sup> + 14 68 <sup>2+</sup> → 27 <sup>+</sup> + 41 <sup>+</sup> 41 <sup>+</sup> → 40 <sup>+</sup> + 1	-3.07
			82 <sup>2+</sup> → 41 <sup>+</sup> + 41 <sup>+</sup> 41 <sup>+</sup> → 13 <sup>+</sup> + 28 41 <sup>+</sup> → 40 <sup>+</sup> + 1	-3.07
			82 <sup>2+</sup> → 41 <sup>+</sup> + 41 <sup>+</sup> 41 <sup>+</sup> → 13 <sup>+</sup> + 28 41 <sup>+</sup> → 40 <sup>+</sup> + 1	-3.07

species change very little from one molecule to the other. The N<sub>1s</sub> Auger and deexcitation spectra are very broad and extend in a large energy range, showing that the molecular ion is produced in an enormous amount of final states. The Auger spectrum of *s*-triazine, for example, shows a broad and intense band, with an onset around the double-ionization threshold (25 eV) extending some 10 eV above. The *s*-tetrazine molecule ionization potential has an electronic structure very close to the *s*-triazine one,<sup>51</sup> and the double-ionization onset lies in the same photon energy range. Consequently, the electronic decay of the N<sub>1s</sub> (and probably the C<sub>1s</sub>) is likely to produce some dicationic states with low internal energy.

Interestingly, the low-energy part (on a binding energy scale) of the deexcitation spectrum of the N<sub>1s</sub> → π\* core-excited *s*-triazine molecule shows<sup>50</sup> that the molecule decays through both spectator and nonspectator transitions. The latter refers to normal electronic autoionization for which the π\* electron participates in the transition and produces a singly charged ion

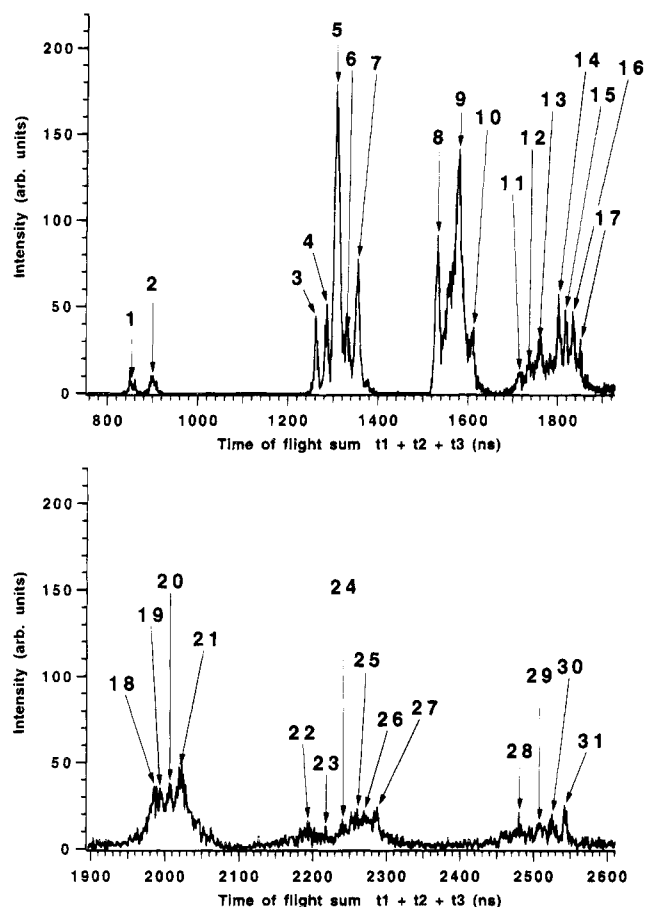


**Figure 3.** One-dimensional spectrum of triple-coincidence spectra ( $t_1 + t_2 + t_3$ ). Each peak number refers to one reaction, as reported in Table 3.

species. According to the spectrum of ref 48, the single-ionization part (below 25 eV binding energy) represents a significant part of the total mass spectrum, and it is probable that there is some contributions of singly charged ion fragments (not counted separately in multicoincidence counts) which are associated with neutral species as is normally found for dissociative single-ionization events.<sup>31</sup>

Up to now, we have considered the fragmentation routes of the dication. In order to identify the third fragment in those cases where it carries a positive charge, we have performed PE3PICO measurements at 285.2 eV photon energy. We have verified that we obtain the same spectrum at other energies near the nitrogen edge, and we show in Figure 3 a one-dimensional representation of triple coincidences, i.e. as a function of the sum of the time of flights for the three correlated ions. Knowing the time of flight of all fragments, from simple PEPICO spectra, and also knowing the correlated fragment pairs of three- and many-body reactions from the PEPICO results, we have been able to identify, for each peak, the values of  $m/z$  of the three correlated fragments, as reported in Table 3. The sum of the three correlated fragments is often not equal to the parent ion mass. Only two peaks (28 and 31) are pure three-body reactions (no undetected fragment) and can be seen as the result of Coulombic explosion. All other processes are four-, five-, and six-body reactions. We have made an attempt to identify the undetected fragments using very simple reasoning. The missing fragments are taken as a stable molecule and/or an atom, following our work on the dissociation of the *s*-tetrazine dication, formed by photon excitation of the neutral molecule near threshold.<sup>32</sup> We have favored first the formation of the biggest species as long as it is a stable neutral molecule or a known

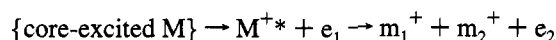
**TABLE 3: Identification of Multifragmentation Processes in *s*-Tetrazine, Associated with the Formation of Three Ionic Fragments, As Measured by PE3PICO at 285.2 eV**

peak number	first ion	second ion	third ion	suggested assignment of undetected fragment
1	H <sup>+</sup>	H <sup>+</sup>	C <sup>+</sup>	C, N <sub>2</sub> , N <sub>2</sub>
2	H <sup>+</sup>	H <sup>+</sup>	N <sup>+</sup>	CN, N <sub>2</sub> , C
3	H <sup>+</sup>	C <sup>+</sup>	C <sup>+</sup>	2N <sub>2</sub> , H <sup>+</sup> or N <sub>2</sub> , N <sub>2</sub> H <sup>+</sup>
4	H <sup>+</sup>	C <sup>+</sup>	CH <sup>+</sup>	2N <sub>2</sub>
5	H <sup>+</sup>	C <sup>+</sup>	N <sup>+</sup>	HCN, N <sub>2</sub>
6	H <sup>+</sup>	CH <sup>+</sup>	N <sup>+</sup>	N <sub>2</sub> , CN or N <sub>2</sub> , CN <sup>+</sup>
7	H <sup>+</sup>	N <sup>+</sup>	N <sup>+</sup>	HCN, CN or N <sub>2</sub> , CH <sup>+</sup> , C
8	H <sup>+</sup>	C <sup>+</sup>	CN <sup>+</sup>	N <sub>2</sub> , NH <sup>+</sup> or N <sub>2</sub> H <sup>+</sup> , N
9sh	H <sup>+</sup>	C <sup>+</sup>	HCN <sup>+</sup>	N <sub>2</sub> , N
	H <sup>+</sup>	CH <sup>+</sup>	CN <sup>+</sup>	N <sub>2</sub> , N
9	H <sup>+</sup>	N <sup>+</sup>	CN <sup>+</sup>	N <sub>2</sub> , CH <sup>+</sup> or HCN + N <sup>+</sup>
10	H <sup>+</sup>	N <sup>+</sup>	N <sub>2</sub> <sup>+</sup>	HCN, C or CN + CH
11	H <sup>+</sup>	C <sup>+</sup>	CHN <sub>2</sub> <sup>+</sup>	N <sub>2</sub>
12	H <sup>+</sup>	CH <sup>+</sup>	CN <sub>2</sub> <sup>+</sup>	N <sub>2</sub>
13	H <sup>+</sup>	N <sup>+</sup>	CHN <sub>2</sub> <sup>+</sup>	CN
14	H <sup>+</sup>	CN <sup>+</sup>	CN <sup>+</sup>	H <sub>2</sub> H <sup>+</sup> or N <sub>2</sub> + H (or H <sup>+</sup> )
15	H <sup>+</sup>	CN <sup>+</sup>	HCN <sup>+</sup>	N <sub>2</sub>
16	H <sup>+</sup>	CN <sup>+</sup>	N <sub>2</sub> <sup>+</sup>	HCN
17	H <sup>+</sup>	HCN <sup>+</sup>	N <sub>2</sub> <sup>+</sup>	CN
18	H <sup>+</sup>	CN <sup>+</sup>	CHN <sub>2</sub> <sup>+</sup>	N
19	H <sup>+</sup>	CN <sup>+</sup>	CN <sub>2</sub> <sup>+</sup>	N
20	H <sup>+</sup>	N <sub>2</sub> <sup>+</sup>	CN <sub>2</sub> <sup>+</sup>	CH
21	H <sup>+</sup>	N <sub>2</sub> <sup>+</sup>	CHN <sub>2</sub> <sup>+</sup>	C
22	CH <sup>+</sup>	N <sup>+</sup>	CN <sub>2</sub> <sup>+</sup>	N, H
23	CH <sup>+</sup>	N <sup>+</sup>	CHN <sub>2</sub> <sup>+</sup>	N
24	N <sup>+</sup>	N <sup>+</sup>	CHN <sub>2</sub> <sup>+</sup>	CH
25	N <sup>+</sup>	CN <sup>+</sup>	CN <sup>+</sup>	N, H, H
26	N <sup>+</sup>	CN <sup>+</sup>	HCN <sup>+</sup>	N, H
27	N <sup>+</sup>	HCN <sup>+</sup>	HCN <sup>+</sup>	N
28	C <sup>+</sup>	N <sub>2</sub> H <sup>+</sup>	CHN <sub>2</sub> <sup>+</sup>	
29	CN <sup>+</sup>	CN <sup>+</sup>	N <sub>2</sub> <sup>+</sup>	H, H
30	CN <sup>+</sup>	HCN <sup>+</sup>	N <sub>2</sub> <sup>+</sup>	H
31	HCN <sup>+</sup>	HCN <sup>+</sup>	N <sub>2</sub> <sup>+</sup>	

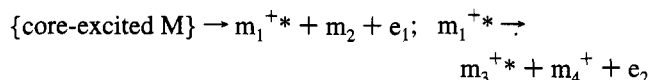
stable ion. In some cases, we have invoked some ionic species such as N<sub>2</sub>H<sup>+</sup>, knowing the large proton affinity of N<sub>2</sub>. In all the other cases we have considered the formation of atomic species. Therefore, on the basis of Table 2, undetected fragments are probably ionic species, and we cannot exclude the existence of dissociative quadruple (and higher) ionization pathways. The main result of the identification of dissociative triple ionization is that this is an important route for the production of H<sup>+</sup>.

**D. Role of Dissociative Autoionization.** The overall ensemble of two-, three-, and many-body reactions presented here has been made by ignoring the nature of the electron relaxation responsible for the dication formation. The fragmentation pattern, which involves both double- and triple-ionization events, is found to be quasi identical at the  $\pi^*$  and  $\sigma^*$  resonances at the carbon 1s or nitrogen 1s edge, despite the different nature of the electronic relaxation of the core hole. In the case of a core-ionized molecule, the normal Auger decay which occurs on a femtosecond time scale, i.e. 80 meV (8 fs) for carbon and 90 meV (7 fs) for nitrogen,<sup>42</sup> is an autoionization process occurring after the ejection of a core electron. Higher order processes known as Auger cascades<sup>1,49</sup> are responsible for the ejection of two or more Auger electrons. In the case of a core-excited ( $C_{1s} \rightarrow \pi^*$ ) molecule, the situation is more complex. It is known<sup>1,52</sup> that the first-order relaxation processes are autoionization processes in which the core-excited electron acts as a spectator or a participator to the transition and, to first order, produces a monocation in a large manifold of electronic states. Double-ionization events are second-order processes such as shake off and two-step autoionization.<sup>52</sup> In molecules, such electronic relaxation processes are intimately related to dissociation. According to detailed measurements on the CO

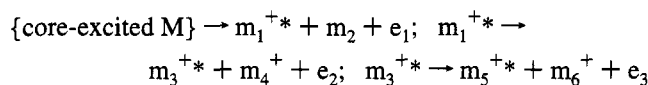
molecule,<sup>37,53,54</sup> the ejection of two electrons is intimately related to fragmentation through dissociative autoionization such as



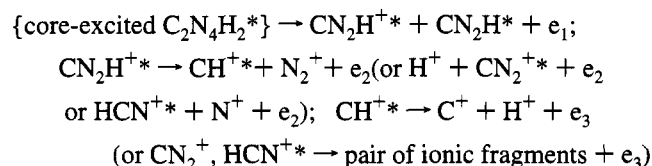
and/or



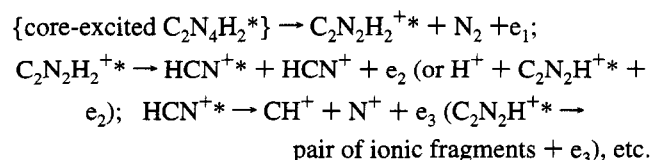
We suggest that higher order processes such as



may also exist. Firstly, the electronic deexcitation spectrum of a core-excited molecule extends over such a wide energy scale that the mono-, di-, and trication carry also a large range of internal energy, so that such a cascade is energetically possible. Note that the double-ionization and triple onsets are generally given by empirical rules<sup>55,56</sup> as respectively 2.8 and 5.6 times the first ionization energies. The deexcitation spectrum of core-excited *s*-tetrazine is not available at this time, but those of isoelectronic azabenzene molecules (benzene rings with one, two, or three nitrogen atoms) have been measured by Eberhardt et al.<sup>50</sup> at the  $N_{1s} \rightarrow \pi^*$  resonance together with the Auger spectrum. A close resemblance between molecules is observed because the electronic structure of these molecules is also similar.<sup>52</sup> Taking the *s*-triazine deexcitation spectrum as a reference because the first ionization energy is close to those of *s*-tetrazine, it is observed<sup>50</sup> that the deexcitation spectrum of the  $N_{1s} \rightarrow \pi^*$  resonance is as smooth as the Auger spectrum and extends beyond the first (9.2 eV, ref 33), second (26 eV, ref 34), and third (52 eV, as estimated from the empirical rule of ref 56) ionization onsets of the molecule. Secondly, numerous dissociation pathways are found (not reported here) to lie at lower energy than the single-, double-, and triple-ionization onset. Thirdly, among the complex manifold of potential surfaces of the mono-, di-, and trication, a great deal are likely to be repulsive at least in the first stage of the fragmentation and favors the occurrence of rapid direct dissociation, on the time scale of autoionization. In the present case, we suggest using for example two important routes discussed in section C, which may exist under the following forms:



or



Similar suggestions can be made for the core-excited molecule but with the double-ionization continua populated first. It is interesting to notice that such dissociative autoionization mechanisms are not contradictory with the suggestions of section C based on the measured slopes of the coincidence peaks, since

the only difference is the additional positive charge on the neutral fragment found among the final products.

Such a description can only account for fast cascades of fragmentations of highly electronically excited ions, on the subpicosecond time scale. If long-lived intermediates such as  $\text{CN}_2\text{H}^+$ ,  $\text{C}_2\text{N}_2\text{H}_2^{2+}$ , and  $\text{C}_2\text{N}_3\text{H}_2^{2+}$  are formed after primary fast fragmentation steps, then statistical rules may apply. Calculations of mass spectra, taking into account the ground state geometries of such intermediate ions,<sup>57</sup> like those performed on core-excited halogeno alkanes by Salman et al.<sup>58</sup> would be of great interest.

**E. Absence of Site Selectivity.** One of the striking observations of this work is that the multicoincidence spectra are quasi identical from one resonance to the other near the carbon and nitrogen edges. The only difference is found in the overall intensity of the spectra from below the edge ( $\pi^*$  resonances) to above ( $\sigma^*$  resonances). This is due to the difference in the degree of ionization which departs from 1 (below the edge) or from 2 (above the edge), as one generally finds in all molecules (see refs 11 and 18, as examples). The quasi identical multicoincidence spectra at photon energies near the carbon and nitrogen resonances require that the localization of the charges after the Auger decay is rapidly lost or that during the sequence of fragmentation reactions there is at least a slow step and/or there are fast bond rupture steps, all favoring the loss of memory of the selected site.

Direct evidence for the charge localization after the core hole decay is given by the differences between the carbon KVV or nitrogen KVV Auger spectra. Unfortunately, the carbon KVV spectrum has not been measured in azabenzene molecules in order to compare with the nitrogen KVV spectra of Eberhardt et al.<sup>50</sup>

We concentrate on the fast dissociation phenomena, i.e., direct processes that are comparable to the lifetime of the core vacancy and proceed on a subpicosecond time scale (see section D). In the first place, the core-excited neutral molecule is highly unstable. The core equivalent molecule at the  $\pi^*$  resonance near the carbon 1s edge is  $\text{CH}_2\text{N}_5$  and near the nitrogen edge is  $\text{C}_2\text{H}_2\text{N}_3\text{O}$ . They have no aromatic character and should be described with repulsive surfaces along the C–C or N–N coordinates, especially those which lead to the opening of the ring. This provides an impulse to open the original ring in the first femtoseconds of the electronic relaxation. The symmetry of the system is such that none of the carbon nor nitrogen sites are favored at this point, especially through the symmetric  $\text{CN}_2\text{H}^+ + \text{CN}_2\text{H}^+$  or the loss of  $\text{N}_2$  from the parent dication giving  $\text{C}_2\text{N}_2\text{H}_2^{2+}$ . Secondly, the residual ions (mono-, di-, and trication) are found to fragment efficiently to produce mainly atomic diatomic species because a significant part of the excess energy is carried as internal energy of the fragments, the rest being found in the kinetic energy of the electrons and the fragments. The probable intimate relation between fragmentation and autoionization favors the delocalization of the charges and occasionally the proton transfer as we have observed. Furthermore, the existence of long-lived intermediates built with both carbon and nitrogen atoms contributes to the loss of memory in the final mass spectrum.

#### IV. Conclusions

The fragmentation of the core-excited *s*-tetrazine molecule can be seen as the result of dissociative single-, double-, and triple-ionization phenomena. The molecule is found to explode via fast sequences of two- and three-body dissociation reactions of the dication and trication, leading primarily to the formation



of atoms and diatomic fragments. The kinetic energy released found in the fragments is fairly small compared to the total energy dumped into the system. This is because (i) the electron ejected in the early stage of the relaxation of the core hole or during the fragmentation carries away most of the excess energy and (ii) the native fragments produced in the early stages of the fragmentation are formed with sufficient internal energy to undergo multifragmentation.

The role of sequential dissociative autoionization associated with the population of single-, double-, and triple-ionization continua is invoked on the basis of the deexcitation electronic and Auger spectra of core-excited azabenzene molecules<sup>50</sup> and probable repulsive surfaces of the residual ionic states.

The lack of site selectivity in the fragmentation is explained by symmetry considerations for the fast fragmentation steps (opening of the cycle and/or first two-body dissociation) and because the first native fragments may undergo statistical fragmentation reactions. However, we cannot rule out the early delocalization of the charge after the core hole relaxation, and final conclusions on this point require measurements of the carbon and nitrogen Auger spectra of this molecule.

**Acknowledgment.** We are grateful to C. Reynaud for illuminating discussions. We are indebted to the LURE staff for operating the storage ring and for general facilities.

## References and Notes

- Nenner, I.; Morin, P. In *VUV and Soft X-ray Photoionization Studies*; Becker, U., Shirley, D. A., Eds.; Plenum Publishing Corp.: London, in press.
- Müller-Dethlefs, K.; Sander, M.; Chewter, L. A.; Schlag, E. W. *J. Phys. Chem.* **1984**, *88*, 6098.
- Murakami, J.; Nelson, M. C.; Anderson, S. L.; Hanson, D. M. *J. Chem. Phys.* **1986**, *85*, 5755.
- Morin, P.; Nenner, I. *Phys. Rev. Lett.* **1986**, *56*, 1913.
- Dujardin, G.; Hellner, L.; Winkoun, D.; Besnard, M. *J. Chem. Phys.* **1986**, *105*, 291.
- Morin, P.; de Souza, G. G. B.; Nenner, I.; Lablanquie, P. *Phys. Rev. Lett.* **1986**, *56*, 131.
- De Souza, G. G. B.; Morin, P.; Nenner, I. *J. Chem. Phys.* **1985**, *83*, 492.
- Nenner, I.; Morin, P.; Simon, M.; Lablanquie, P.; de Souza, G. G. B. In *Desorption Induced by Electronic Transitions*, DIET III, Springer Series in Science Vol. 13; Stulen, R. H., Knotek, M. L., Eds.; Springer Verlag: Berlin, 1988; pp 10–31.
- Nagaoka, S.; Koyano, I.; Ueda, K.; Shigemasa, E.; Sato, Y.; Yagishita, A.; Nagata, T.; Hayaishi, T. *Chem. Phys. Lett.* **1989**, *154*, 363.
- Morin, P.; LeBrun, T.; Lablanquie, P. *J. Chim. Phys. (France)*, **1989**, *86*, 1833.
- Lablanquie, P.; Souza, A. C. A.; de Souza, G. G. B.; Morin, P.; Nenner, I. *J. Chem. Phys.* **1989**, *90*, 7078.
- Morin, P.; LeBrun, T.; Lablanquie, P. *Bull. Sté Royale Sci. Liège* **1989**, *58*, 135.
- Ueda, K.; Shigemasa, E.; Sato, Y.; Nagaoka, S.; Koyano, I. *Chem. Phys. Lett.* **1989**, *154*, 357.
- Lapiano-Smith, D. A.; Ma, C. I.; Wu, K. T.; Hanson, D. M. *J. Chem. Phys.* **1989**, *90*, 2162.
- Ueda, K.; Shigemasa, E.; Sato, Y.; Nagaoka, S.; Koyano, I.; Yagishita, A.; Hayaishi, T. *Phys. Scr.* **1990**, *41*, 78.
- Ueda, K.; Sato, Y.; Nagaoka, S.; Koyano, I.; Yagishita, A.; Hayaishi, T. *Chem. Phys. Lett.* **1990**, *170*, 389.
- Ueda, K.; Shigemasa, E.; Sato, Y.; Nagaoka, S.; Koyano, I.; Yagishita, A.; Hayaishi, T. *Chem. Phys. Lett.* **1990**, *166*, 391.
- Sato, Y.; Ueda, K.; Yagishita, A.; Sasaki, T.; Nagata, T.; Hayaishi, T.; Yoshino, M.; Koisumi, T.; Itoh, Y.; MacDowell, A. A. *Phys. Scr.* **1990**, *41*, 55.
- Habenicht, W.; Baiter, H.; Müller-Dethlefs, K.; Schlag, E. W. *J. Phys. Chem.* **1991**, *95*, 6774.
- Imamura, T.; Brion, C. E.; Koyano, I.; Ibuki, T.; Masuoka, T. *J. Chem. Phys.* **1991**, *94*, 4936.
- Morin, P.; Lavollée, M.; Simon, M. In *Proceedings of the 10th International Conference on Vacuum Ultra-Violet and Radiation Physics*, Paris, July 27–31, 1992; Willeumier, F. J., Petroff, Y., Nenner, I., Eds.; World Scientific: Singapore, 1993; pp 211–225.
- Morin, P.; Lavollée, M.; Meyer, M.; Simon, M. In *Proceedings of the XVIII International Conference on the Physics of Electronic and Atomic Collisions*, ICPEAC AIP 295; Andersen, T., Fastrup, B., Folkmann, F., Knudsen, H., Andersen, N., Eds.; 1993; pp 139–151.
- LeBrun, T.; Lavollée, M.; Simon, M.; Morin, P. *J. Chem. Phys.* **1993**, *98*, 2534.
- Nagaoka, S.; Ohshita, J.; Ishikawa, M.; Masuoka, T.; Koyano, I. *J. Phys. Chem.* **1993**, *97*, 1488.
- Simon, M.; LeBrun, T.; Martins, R.; de Souza, G. G. B.; Nenner, I.; Lavollée, M.; Morin, P. *J. Phys. Chem.* **1993**, *97*, 5228.
- Schmelz, H. C.; Reynaud, C.; Simon, M.; Nenner, I. *J. Chem. Phys.* **1994**, *101*, 3742.
- Baer, T. *Adv. Chem. Phys.* **1986**, *64*, 111.
- Casanova, S.; Montmerle, T.; Feigelson, E. D.; André, P. *Astrophys. J.*, in press.
- Chetioui, A.; Despinay, I.; Guiraud, L.; Adaoui, L.; Sabatier, L.; Dutrillaux, B. *Int. J. Radiat. Biol.*, in press.
- Nahon, L.; Morin, P.; Larzillière, M.; Nenner, I. *J. Chem. Phys.* **1992**, *96*, 3628.
- Nenner, I.; Dutuit, O.; Richard-Viard, M.; Morin, P.; Zewail, A. H. *J. Am. Chem. Soc.* **1988**, *110*, 1093.
- Nenner, I.; Eland, J. H. D. *Z. Phys. D.* **1992**, *25*, 47.
- Frasinsky, L. J.; Stankiewicz, M.; Randall, K. J.; Haterley, P. A.; Codling, K. *J. Phys. B* **1986**, *19*, L819.
- Eland, J. H. D. *Mol. Phys.* **1987**, *61*, 725.
- Simon, M.; LeBrun, T.; Morin, P.; Lavollée, M.; Maréchal, J. L. *Nucl. Instrum. Methods* **1991**, *B62*, 167.
- Sirotti, F.; Toscano, S.; Waldhauer, A.; Rossi, G. *Synchrotron Radiation: Selected Experiments in Condensed Matter Physics*; Monte Verita, Ed.; Birkauer, Verlag: Basel, 1990.
- Hitchcock, A. P.; Lablanquie, P.; Morin, P.; Lizon à Lugrin, E.; Simon, M.; Thiry, P.; Nenner, I. *Phys. Rev. A* **1988**, *37*, 2448.
- Eland, J. H. D. *Laser Chem.* **1993**, *11*, 259.
- Eland, J. H. D. *Vacuum Ultraviolet Photoionization and Photo-dissociation of Molecules and Clusters*; Ng, C. Y., Ed.; World Scientific: Singapore, 1991; pp 397–343.
- Antonius, T.; Marcelis, M.; van der Plas, H. C. *J. Heterocycl. Chem.* **1987**, *24*, 545.
- Horsley, J. A.; Stöhr, J.; Hitchcock, A. P.; Newbury, D. C.; Johnson, A. L.; Sette, F. *J. Chem. Phys.* **1985**, *83*, 6099.
- Stöhr, J. *NEXAFS Spectroscopy*, Springer Series in Surface Science No. 25; Springer Verlag: Berlin, 1992.
- Schwarz, W. H. F.; Chang, T. C.; Seeger, U.; Hwang, K. H. *Chem. Phys.* **1987**, *117*, 73.
- Aminpirooz, S.; Becker, L.; Hillert, B.; Haase, J. *Surf. Sci.* **1991**, *244*, L152.
- Nenner, I.; Schulz, G. J. *J. Chem. Phys.* **1975**, *62*, 1747.
- Innes, K. K.; Byrne, J. P.; Ross, I. G. *J. Mol. Spectrosc.* **1967**, *22*, 125.
- Chen, C. T.; Ma, Y.; Sette, F. *Phys. Rev. A* **1989**, *40*, 6737.
- Simon, M.; Lavollée, M.; Meyer, M.; Morin, P. *J. Chim. Phys. (France)* **1993**, *90*, 1325.
- Lavollée, M. Private communication.
- Eberhardt, W.; Dudde, R.; Rocco, M. L. M.; Koch, E. E.; Bernstorff, S. *J. Electron. Spectrosc. Relat. Phenom.* **1990**, *51*, 373.
- Von Niessen, W.; Kralmer, W. P.; Diercksen, G. H. F. *Chem. Phys.* **1979**, *41*, 113 and references therein.
- Nenner, I.; Morin, P.; Lablanquie, P. *Comments Atom. Mol. Phys.* **1988**, *14*, 203.
- Eberhardt, W.; Plummer, E. W.; Chen, C. T.; Ford, W. K. *Aust. J. Phys.* **1986**, *39*, 853.
- Becker, U.; Hemmers, O.; Langer, B.; Menzel, A.; Wehlitz, R.; Peatman, W. B. *Phys. Rev. A* **1992**, *45*, R1295.
- Tsai, B. P.; Eland, J. H. D. *Int. J. Mass Spectrom. Ion Phys.* **1980**, *36*, 143.
- King, G.; Tronc, M.; Read, F. H.; Bradford, R. C. *J. Phys. B* **1977**, *10*, 2479.
- Auimon, M. F.; Gonbeau, D.; Suburu, F.; Pfister-Guillouzo, G. Private communication.
- Salman, I.; Silberstein, J.; Levine, R. D. *J. Phys. Chem.* **1991**, *95*, 6781.